TECHNIKA TRANSPORTU SZYNOWEGO

Roman BOGACZ, Kurt FRISCHMUTH

SELECTED PROBLEMS OF WAVE PHENOMENA IN CATENARIES

Abstract

Wave phenomena in one-dimensional media caused by moving forces are discussed with special emphasis on application to the interaction between pantograph and traction. Stationary solutions are examined in the case of unbounded domains along with boundary effects in the case of finite domains. The influence of the travelling speed on stability is examined. In more complex structures, numerical methods are used to find maximal deflections.

INTRODUCTION

The energy supply to an electrical locomotive or to EMU trains is dependent on the contact between pantographs and traction wire [1,10-12]. Since the train, in general, is moving with a certain speed, the force is generating dynamic deflections in the traction [5-7]. These are propagating along the wire, being reflected at supports and boundaries, causing nontrivial interactions with the pantograph.

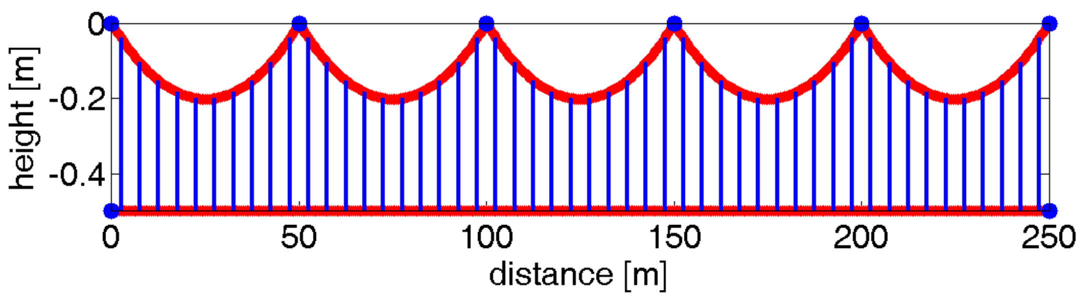

Fig. 1. Segment of (simplified) traction

In order to minimize fluctuations, a messenger wire is spanned above the actual contact wire, which is periodically suspended by droppers holding it at the desired level. Consequently, there will be waves running in both wires, which are coupled at the positions of the droppers. A typical layout is presented in Fig. 1.

Before we will start numerical studies on the two-wire case, let us collect some facts about wave propagation due to moving forces in a single wire, modeled as a string.

1. ANALYTICAL SOLUTIONS

We start our investigation from the classical case of the wave equation as in [2,5,6]

$$(Su(x,t)''+Pu(x,t))''+\rho\ddot{u}(x,t)=f(x,t) \quad (1)$$

Here we denote by *S* the bending stiffness of the medium, by *ρ* the mass density per unit of length and by *P* the compressing force. Time is denoted by *t*, position along the wire by *x*, the corresponding partial derivatives are indicated by a superposed dot or an apostrophe, correspondingly. The external force *f* may be modeled as a Dirac distribution, which is concentrated in each moment *t* at the point *Vt*, where *V* is the travelling speed of the pantograph. In a typical traction wire, *S* may be well neglected in a first approximation, and *P* is negative. Technically, the tension is maintained by concrete weights of about two metrical tons of mass. This leads in the case of very flexible media to the simplified equation

$$\ddot{u}(x,t)-c^2u(x,t)''=f(x,t)/\rho \quad (2)$$

We introduced c^2 for the ratio of tension *P* to mass density. Notice that often, instead of *P*, in the literature on beams there appears the parameter *T* (for tension). We prefer to reserve *T* for the duration of transient processes, and hence use the parameter name *P* as typically in papers on columns.

1.1. Unbounded case

Solutions to this hyperbolic partial differential equation of second order can be obtained in terms of the initial deflections and integrals over initial speed and external force.

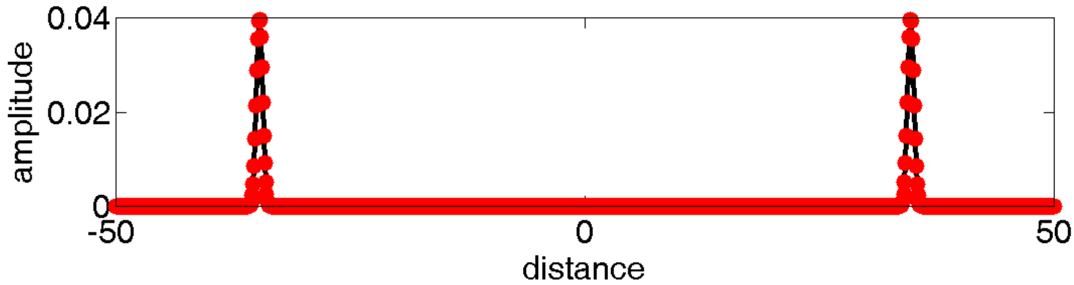

Fig. 2. Classical wave solution

Assuming constant coefficients and zero forces, any solution of (2) on the whole real axis $x\in R$ has the form

$$u(x,t)=\phi(x+ct)+\psi(x-ct) \quad (3)$$

An initial concentrated shift around the origin splits into two waves, one running left, the other right, with equal but opposite speeds, see Fig. 2. The functions Φ and Ψ can be identified from initial conditions $u(\cdot,0)$ on the deflection and on the initial lateral speed $v(\cdot,0)=\dot{u}(\cdot,0)$.

In the relevant case of a nontrivial inhomogeneity *f*, i.e., when the disturbance is caused by an external force, the solution *u* at a given position *x* depends at time *t* on the force terms at all positions from which *x* can be reached at wave speed *c* in a time span smaller or equal than *t*. In fact, one obtains

$$u(x,t)=\frac{u_0(x-ct)+u_0(x+ct)}{2}+\frac{1}{2c}\int_{x-ct}^{x+ct}v_0(\xi)d\xi+\frac{1}{2}\int_0^t\int_{x-c(t-\tau)}^{x+c(t+\tau)}f(\xi,\tau)d\xi d\tau \tag{4}$$

where u_0 and v_0 denote initial conditions, defined for all positions.

In the case of an initially undisturbed wire the first two contributions vanish, the solution reduces to the double integral of the source term. Given the small size of the contact area between wire and pantograph, it is sensitive to assume

$$f(x,t)=F(t)\delta(Vt) \tag{5}$$

with δ denoting Dirac's distribution and *F* the magnitude of the vertical force at time *t*. This renders the inner integration trivial – it yields simply $F(\tau)$ or zero. It remains to determine the actual interval of the time integration, where the inner integral is nonzero, i.e., when the travelling force crosses the influence region of the wave equation.

Typically, one assumes a harmonic force function of the form $F(t)=F_m+F_d\sin(\Omega t)$. In that case, the integration can be carried out analytically, and we obtain a closed formula for the solution.

Let us study the special case of $V=c$. In order to calculate the amplitude at a given point (x,t) in the upper half-plane on the trajectory of the force, i.e, for $x=Vt$, we evaluate (4) by inserting the special choice of (5).

$$u(x,t)=\frac{1}{2}\int_0^t F(\tau)d\tau=0.5tF_m+\frac{F_d}{2\Omega}(\cos(\Omega t)-1) \tag{6}$$

Obviously, with running time *t* the deflection at the point of contact grows unboundedly, proportionally to time and mean contact force. The same is true for all travelling speeds, unless a bedding or some supports are added to the setup.

The case $V=c$ is called critical, because for that choice the derivative of the solution under the force becomes infinite, see Figs. 3 and 4.

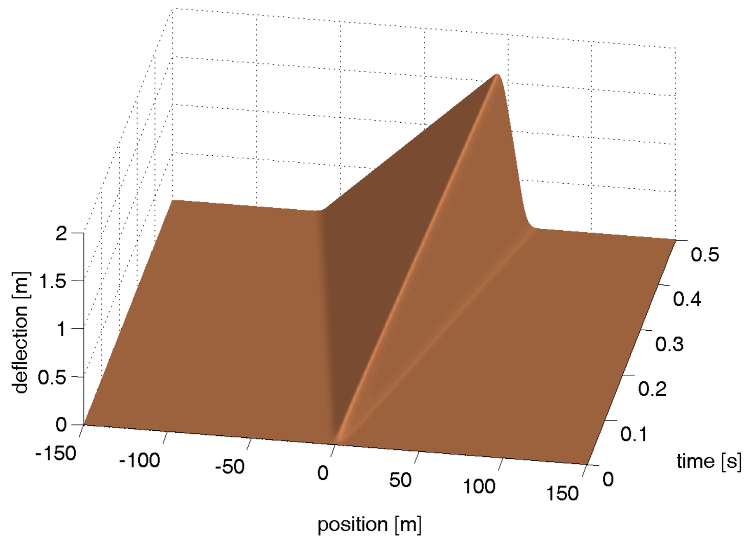

Fig. 3. Solution on t=0 … 0.5s for travelling speed V equal 0.75 times the wave speed c

In Figs. 3 and 4, we assumed a tension of 20kN, and a mass per length of 1.33 kg/m, see [1]. This gives a wave speed of around 120m/s. The lateral force was constant equal to 200N. The travelling speed in Fig. 3 is 320km/h. The unrealistic large values of the deflection are, obviously a consequence of the lack of supports and, most of all, the lack of coupling. For realistic values of the static stiffness as function of x cf. [12]. It has to be stressed that the model of a constant or periodic force, while suitable in rail-wheel contact, is unrealistic for a pantograph, [3-6]. Later on we will introduce coupling, e.g. reduce the value of the force in a nonlinear way in dependence on the wire deflection.

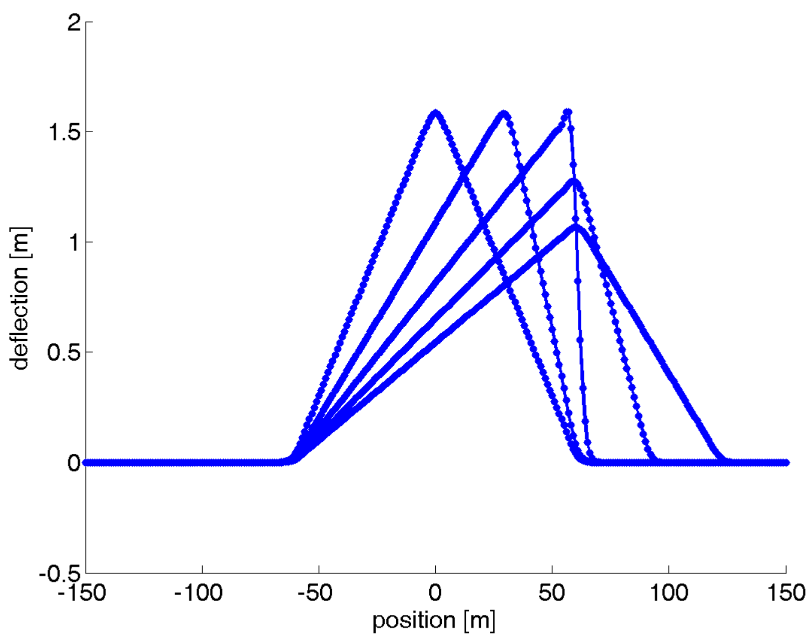

Fig. 4. Solutions at t=0.5s for travelling speed V equal to 0, 0.5, 1, 1.5 and 2 times the wave speed c

Notice that for the original partial differential equation (1), which is of fourth order and non-hyperbolic, but degenerated parabolic, the discussion is more complex. Solutions are found, again, in the form of running waves as in (3), however there is no constant wave speed.

Superpositions of sinusoidal waves, running at a speed depending on their frequencies, have to be considered, see [4,5]. Later we will discuss the magnitude of the dispersion effects by numerical experiments.

1.2. Bounded case

In the case that the position variable x is restricted to a finite interval, $x \in [-L/2, L/2]$, formula (4) is not applicable. Instead, it is assumed that the solution is a sum of product terms of the form

$$u(x,t) = \sum_l a_l(x) b_l(t) \tag{7}$$

Now, substituting (7) into the homogeneous version of (2), one obtains that the amplitudes a have to be sine or cosine functions. Further, they have to obey boundary conditions. In the Dirichlet case, this implies $a_l(x) = \cos(l\pi / L)$. For the time dependence b a second order differential equation is obtained, which together with the initial conditions allows to define the solution to the initial boundary value problem in a unique way as an infinite trigonometric series.

Most essentially, as a consequence of the boundary conditions, we can observe reflections from the boundaries. Under certain circumstances, superpositions of running waves may take the special form of a standing wave.

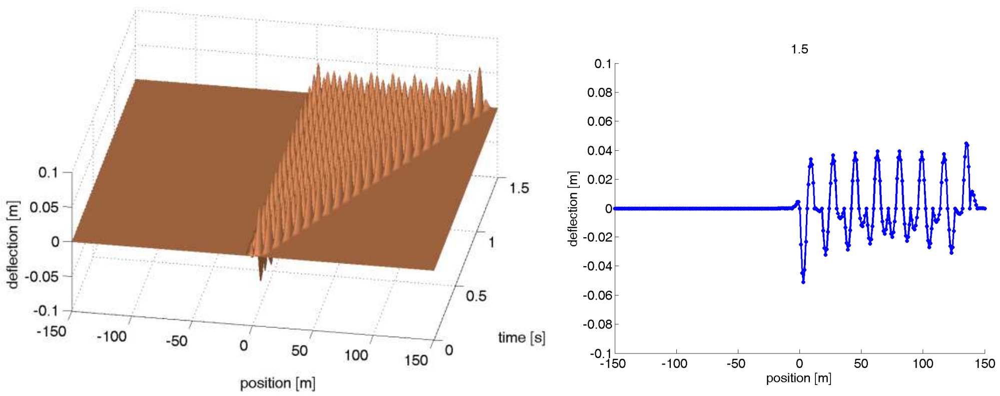

Fig. 5. Solutions for regular rigid supports each 6m

As we can see from Fig. 5, periodic supports block the growth of the amplitude under the force. There are only oscillations in the wake, and the maximal deviation drops to several centimeters. However, this setup is still far from realistic.

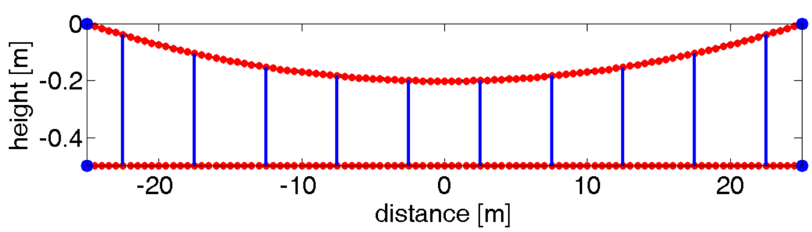

Fig. 6. Geometry of one cell of the studied system

In a more complex structure as e.g. in Fig. 6, which is one cell of the sample layout in Fig. 1, analytical considerations become more and more unpractical due to the large number of reflections overlaying each other. Consequently, it is preferable to switch to numerical approximations. In fact, already the form (7) of an analytical solution – as an infinite series – requires eventually a numerical evaluation. For very concentrated source terms, the convergence of (7) may be less satisfactory than a direct approach by finite elements or by the method of lines.

2. NUMERICAL SOLUTIONS

2.1. Semi-Discretization

One of the most straightforward numerical approaches to the solution of (2) is the substitution of the second order partial differentiation by a second order finite difference. An alternative method was discussed and applied in [2]. Usually we use a uniform grid with stepsize $h = \Delta x = x_{j+1} - x_j = \frac{L}{n}, \quad j = 0, ..., n-1$. We denote by u_j the deflection at the position x_j and by v_j the corresponding velocity. Next, the value of the second order space derivative $u''(x_j)$ is approximated by the difference between u_j and the arithmetic mean between its two closest neighbors, divided over the square of the stepsize

$$u''(x_j, t) \approx \frac{u_{j-1}(t) - 2u_j(t) + u_{j+1}(t)}{h^2} \tag{8}$$

As for the time variable, in numerical calculations we restrict ourselves to a finite set of instants t_0 through t_m as well. However, we do not treat the time derivatives in an analogous way as the space derivative. First of all, equations of second order are converted into systems of twice as many first order equations, in our case for the two unknown *(n+1)*-dimensional vector functions $\dot{u}(t)$ and $\dot{v}(t)$. Next, instead of approximating both time derivatives e.g. by forward differences, the system should be passed to a higher order algorithm for the integration of ordinary differential equations, as *dopri* in the non-stiff case or a *BDF*-scheme in the stiff case, see e.g. [8,9].

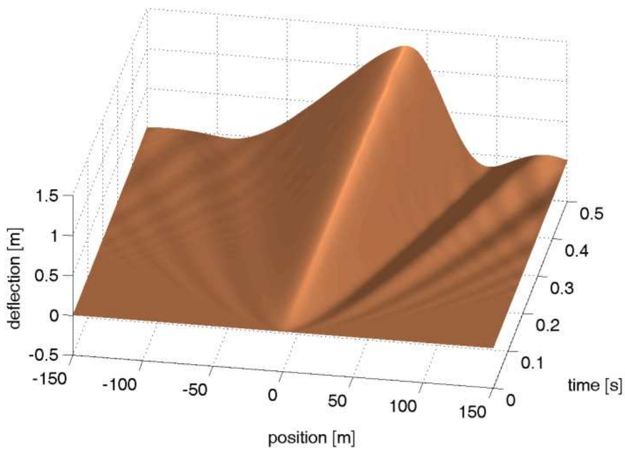

Fig. 7. Solutions for wire with (considerable) bending stiffness

In Fig. 7 we present a solution, where a finite value of the bending stiffness S =200kNm^2 was taken into account. Technically, this is obtained by applying (8) to itself, so that a forth order derivative is calculated from five nodal values. Obviously, in the result there are waves, running much faster, before the front of the hyperbolic limit case. On a bounded domain with hard boundary conditions, reflections interfere with the original wave.

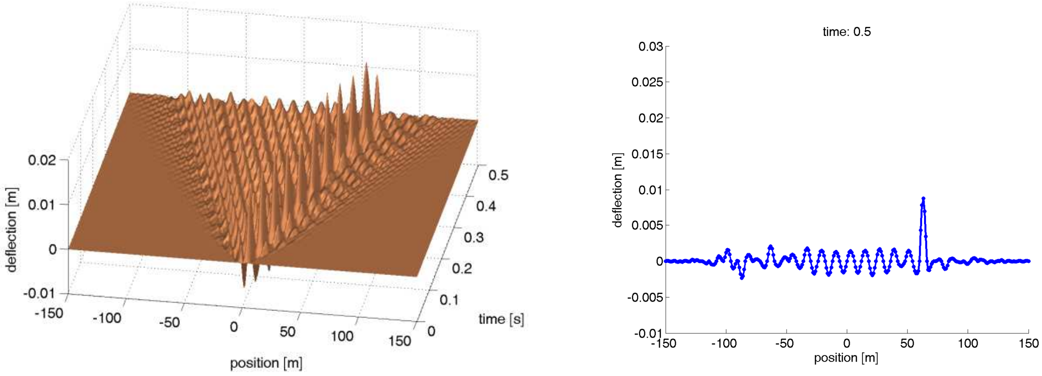

Fig. 8. Solutions for supported wire with bending stiffness

Now, we are able to combine the effects of various supports – periodic or not, mistuning can be handled easily – and non-vanishing bending stiffness. In Fig. 8 we see that for the fourth order equation (1), however small the bending stiffness *S*, waves run ahead of the moving force, even when travelling at the hyperbolic wave speed. As opposed to Fig. 5, also the wake extends to positions behind the starting point of the force, from the origin to the left. However, the small values of the deflection are now due to the hard supports – which are not present in a real catenary system. We will come back to this in Sec. 3.

2.2. Modal Analysis

Until now, the studied system is purely elastic, no energy is dissipated by viscous or frictional forces. Consequently, high frequency oscillations are not damped out, so that solutions to problems with a concentrated and moving force become quickly very noisy, see e.g. [6]. Often this noise is reduced by filtering, e.g. at 20 Hz. Alternatively, we may try to calculate the solution in a form similar to (7), where the amplitude function *a(x)* is replaced by numerically calculated eigenforms of the elastic system, e.g. as depicted in Fig. 1 or Fig. 6. The sum is then cut when the eigenfrequency exceeds the level we are interested in.

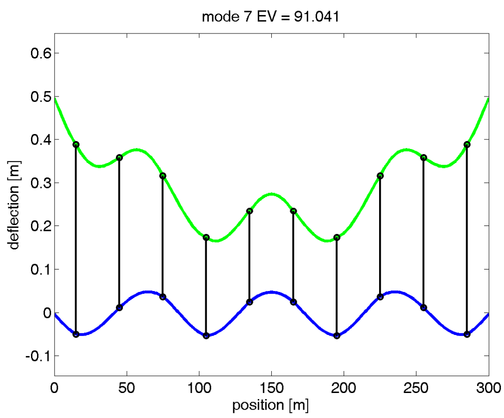

Fig. 9. A symmetric low frequency mode of a considered two-wire system

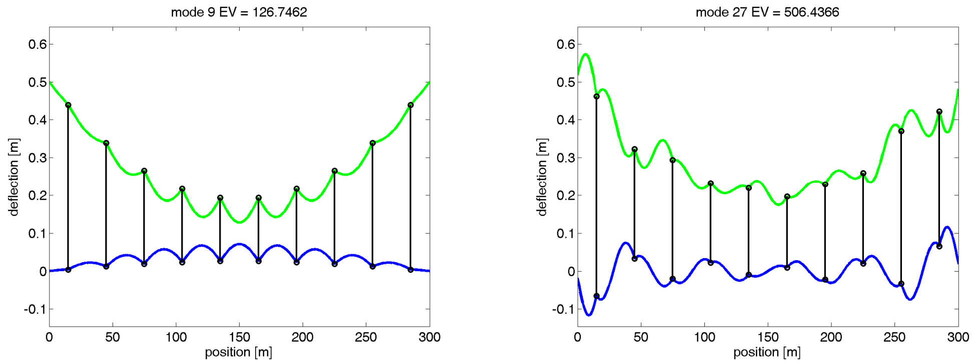

Fig. 10. A symmetric medium (left) and elevated (right) frequency mode of the two-wire system

In Fig. 9 a typical low frequency eigenform is presented. Despite the coupling between two wires, the form is very similar to that of a homogeneous oscillating elastic string. Above a certain frequency, however, eigenmodes are composed piecewise of those of swinging segments, initially all of them in first mode, in the next range second modes appear, see Fig. 10.

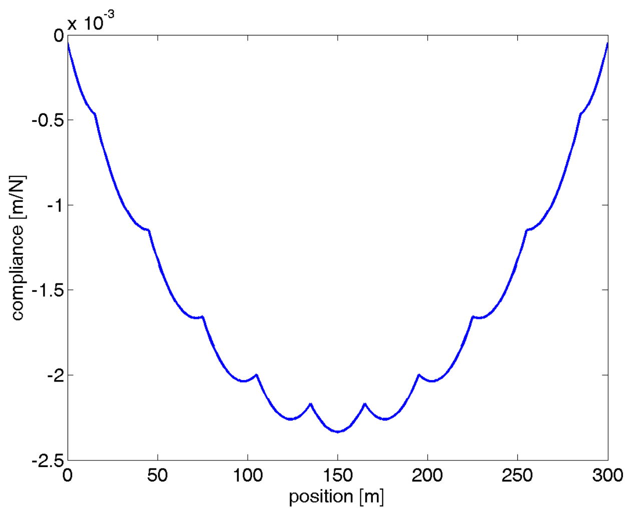

Fig. 11. Response to a concentrated force as function of point of attack

The medium frequencies, at which segments of the wires may oscillate separately in anti-phase, are consistent with parametric excitations due to the variable compliance resulting from the system geometry, see Fig. 11. There we show the deflection caused by a static downward force of 1N, acting on a node on the lower wire, evaluated at the point, where the force is applied.

3. COUPLING

3.1. Wire-Single Pantograph

Until now, the source term causing the disturbance in the catenary was assumed to be known in advance, as a function or distribution on space and time. In such a case, there is obviously no feedback between the wire and the pantograph.

In [7], the pantograph was modeled as a mass-spring system, moving at given speed along the wire. In such a system, the lateral force is no longer pre-assigned, it will be a result of the time integration. Here we restrict ourselves to a force, which decreases with increasing elevation of the wire.

Fig. 12 presents results on the case studied before in Sec. 2, Fig. 3. There are no supports, now, yet the solution stays bounded due to the reaction of the pantograph's contact force, when the wire moves away from it. In the pure string case, the solution is a fuzzy version of the characteristic cone of the hyperbolic problem. When allowing for bending stiffness, again, waves may fun in front and behind that area. We picked a speed of 75% of the wave speed for the forward motion of the locomotive – which is 5% more than usually recommended.

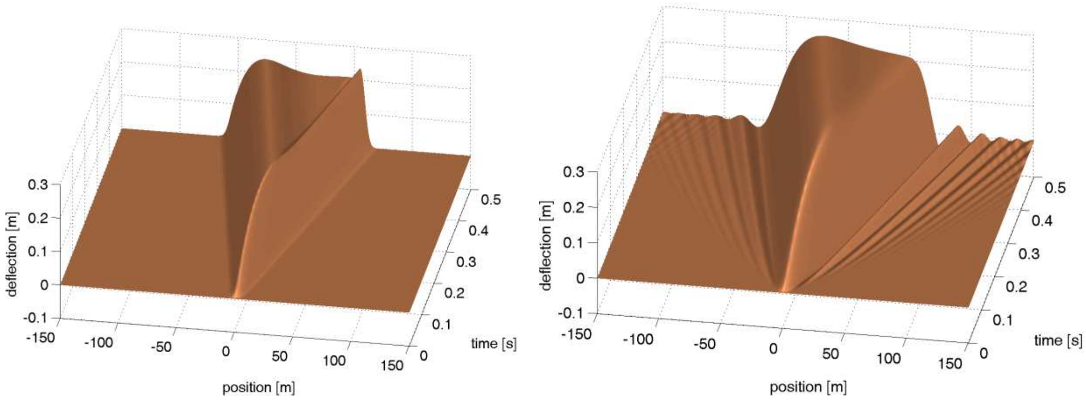

Fig. 12. Solutions for elastic pantograph without and with bending stiffness of contact wire

Now, eventually, we repeat the calculations for the two-wire structure presented in Fig. 6. In Fig 13, the influence of the droppers is clearly seen.

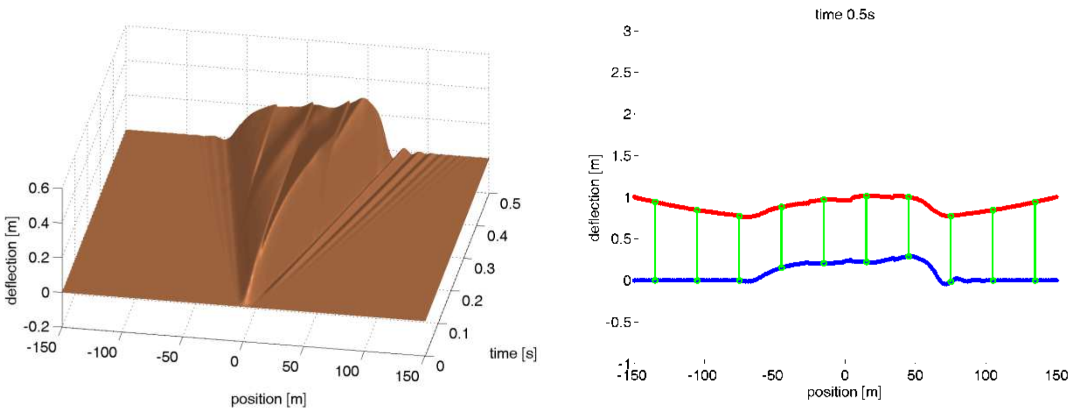

Fig. 13. Solutions for elastic pantograph running on a contact wire attached to a messenger wire

3.2. Wire-Two Pantographs

We come now to the case of several pantographs pressed to the same contact wire. Now, the second one runs into the wake of the leading one, but also disturbances from a trailing pantograph may reach the leading one and cause considerable fluctuations in the contact forces, see Fig. 14. Here we present a numerical result in the case of just two pantographs, running in a distance of 37m. Otherwise, all settings are identical as on the right side of Fig. 13, i.e., we assumed a small bending stiffness, no supports and a decreasing characteristic of the pantographs.

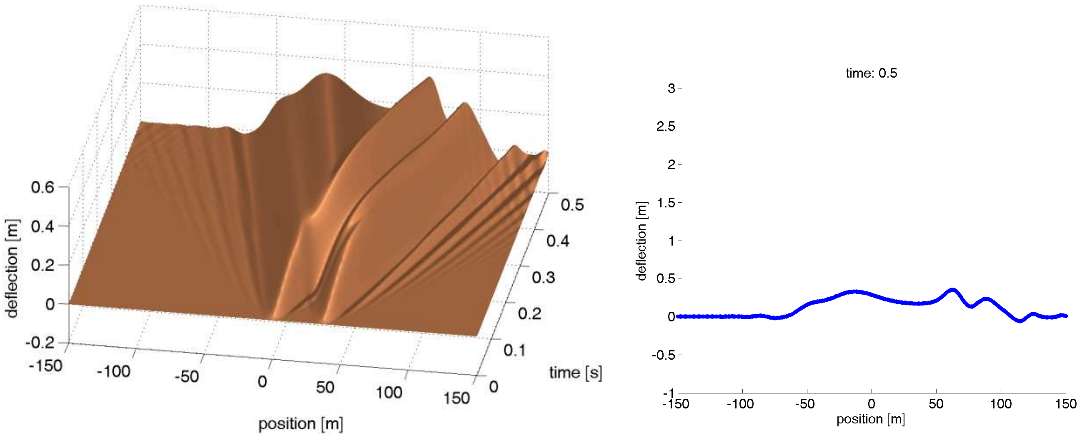

Fig. 14. Solutions for two elastic pantographs running on a bending-stiff contact wire

SUMMARY

In the case of an unbounded flexible string, the behavior of analytical solutions can be studied by evaluation of classical formulas, their stability depends on the relation between traveling and wave speed. For a finite length of wire, the amplitude of deflections is calculated by numerical methods. Again, it depends on the travelling speed, which should remain well below the speed of elastic transversal waves in the wire.

In a next step, the dynamics of the pantograph, modeled as a multi-body system, will be included, so that the traveling force will no longer be pre-assigned but dependent on the solution for the wire deflection. This is of particular importance if multiple pantographs in a short distance between each other are considered. In this matter, recently in [1] results on the value of contact forces were published, see Fig 15.

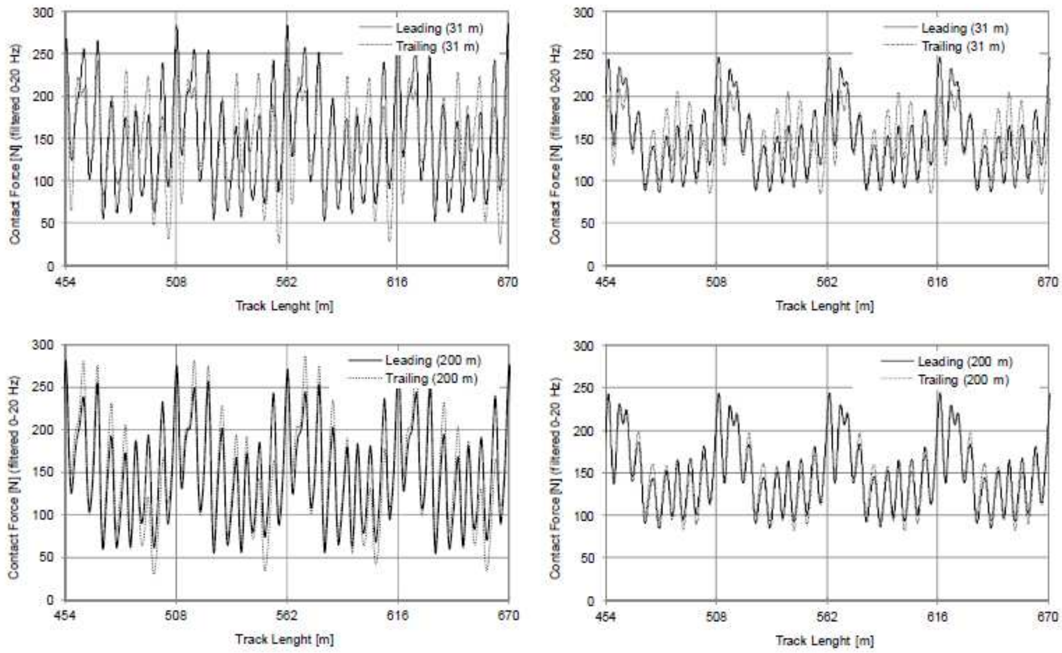

Fig. 15. Contact forces in dependence on wire and pantograph motion [1].

ZJAWISKA FALOWE
W TRAKCJI KOLEJOWEJ

Streszczenie

W artykule dyskutowane są zjawiska falowe spowodowane siłami wędrującymi w ośrodkach ciągłych jednowymiarowych ze szczególnym uwzględnieniem zastosowań do współdziałania odbieraka prądu i trakcji elektrycznej w kolejnictwie. Analizowano rozwiązania stacjonarne w przypadku dziedziny nieograniczonej wraz z efektami brzegowymi przy zagadnieniach na przedziałach skończonych. Zbadano wpływ prędkości ruchomej siły na stabilność. W układach bardziej złożonych używano metod numerycznych w celu obliczenia maksymalnych przesunięć.

BIBLIOGRAFIA

1. Ambrósio J., Pombo J., Pereira M., Antunes P., Mósca A., *A, Computational Procedure for the Dynamic Analysis of the Catenary-Pantograph Interaction in High-Speed Trains,* J. Theoretical and Applied Mechanics, 50, 3, pp. 679-680, 2012
2. Bajer Cz., Bogacz R.: *Dynamic contact problem by the use of the space-time element method*, Proc. of Vth Intern. Symp. On Numerical Methods in Engineering, Lausanne, Switzerland, Springer-Verlag, pp. 313-318, 1989
3. Bogacz R.: *On stability of mutual interaction of oscillator and string in relative motion,* (in Polish), Mechanika Teoret. i Stosow. 4, 14, pp. 519-534, 1976
4. Bogacz R.: Selected *problems of stability of motion of a continuous and discrete systems,* in: The Modern Methods of Stability of Structures, (in Polish), Janowice 1985, pp. 7-75, Ossolineum 1987
5. Bogacz R., Frischmuth K.: *On some new aspects of contact dynamics with application in railway engineering,* J. Theoretical and Applied Mechanics., 50.1, pp. 119-130, Warsaw 2012
6. Bogacz R., Frischmuth K.: *Vibration in Sets of Beams and Plates Induced by Traveling Loads*, Archive of Applied Mechanics, 2009
7. Bogacz, R., Szolc, T., *Analysis of dynamic interaction between the continuous string and moving oscillator,* Eng. Trans, 41, 3–4.1993, pp. 361–380, 1993
8. Frischmuth K.: *On the numerical solution of rail-wheel contact problems*. J. Theoretical and Applied Mechanics, 34, 1, 7–15, 1996
9. Frischmuth K.: *Contact, motion and wear in railway mechanics*, J. Theoretical and Applied Mechanics, 39, 3, 2001
10. Kumaniecka A.: *Dynamics of catenary wire*, Proc. of the German-Polish Workshop Dynamical Problems in Mechanical Systems, Zakopane, September 1-5, 1997
11. Kumaniecka, A., Grzyb, A., *On dynamics of catenary -pantograph modelled as discrete-continuous system,* Machine Dynamics Problems, 24, 1, pp. 105–119, 2000
12. Kumaniecka A., Prącik M., *Modelling of the Catenary Pantograph System*, 2011

Autorzy:

prof. Roman BOGACZ – Politechnika Krakowska

prof. Kurt FRISCHMUTH – Politechnika Koszalińska